LA- UR-01-1476
Approved for public release
distribution is unlimited

TITLE An Unsplit, Two-Dimensional Advection Algorithm (U)

Author(s) S. J. Mosso and B. K. Swartz

Submitted to: This paper was prepared for submittal to
Nuclear Explosives Code Developers
Collaborations (NECDC) 2000
Oakland, CA
October 23 – 27, 2000

Los Alamos
NATIONAL LABORATORY

An Unsplit, Two-Dimensional Advection Algorithm (U)

S. J. Mosso and B. K. Swartz
Los Alamos National Laboratory

This paper describes a method of representing the distribution of advected quantities over zones with a conservative, multi-dimensional, monotonically limited, quadratic interpolant. The method is applicable to two-and three-dimensional, regular and irregular grids. The intent of this method is to reduce dissipation associated with advection. (U)

Keywords: hydrodynamics, advection, remap, link

Introduction

The first author's motivation for this work is contained in this introduction.

Advection packages in Eulerian codes can be broken into two major pieces. The first piece is the geometric calculation of the flux volumes. These volumes describe the physical extent of the material that will be transported from the donor zone to neighboring acceptor zones. It is the first author's opinion that for two spatial dimensions, the flux volume calculation has been effectively and efficiently solved in the two papers 'Reconstructing Volume Tracking' (Rider and Kothe, 1998) and 'Incremental Remapping as a Transport/Advection Algorithm' (Dukowicz and Baumgardner, 2000).

The remaining component of an advection package is the calculation of the conserved quantities that each of the flux volumes carries from its donor to acceptor zones. To this end we propose, for each cell of an irregular grid, a way to use nearby cell mean values to define and then limit a quadratic approximant. The result is a conservative but discontinuous piecewise quadratic approximation.

Most Eulerian and Arbitrary Lagrangian Eulerian (ALE) codes perform material advection through a series of one-dimensional advection steps. As an example, flux split advection for a zone that is uniformly expanding in all directions does not move material through all of its faces in a single step. By stepping the advection calculation through the facial pairs, flow that is diagonal to the facial normals will first be transported out of one face and then through a neighboring face in the acceptor zone. Alternating the order for the direction of advection reduces directional asymmetries.

The volume of material transported across the zone faces in traditional Eulerian codes is calculated using a single-dimensional simplification. The depth of the flux volume is simply the vector dot product of the velocity distribution over the face with the facial normal times the time step. The flux volume is then the facial area times the fluxing depth. No variation of the fluxing depth over the face is considered.

The value of the conserved quantities that the fluxed material carries from the donor zone to the acceptor zone is calculated by using one of two, nearly equivalent, methods: van Leer's (van Leer, 1977) third-order scheme or Boris and Book's Flux Corrected Transport (FCT) (Boris and Book, 1973). In both of these methods, a one-dimensional, monotonic, quadratic distribution is used to represent the spatial variation of each conserved quantity over the donor zone. By monotonic, we mean that the interpolated value at the zone face lies between the mean values of the conserved quantity in the donor zone and those of the corresponding neighbor zone (MUSCL –type monotonicity). As with the

calculation of the flux volume, the spatial variation of the conserved quantity in the directions normal to the facial normal is not accounted for in the quadratic distribution.

Another contributor to grid imprinting is the variation in advection dissipation. In general, the third and higher spatial derivatives of conserved quantities are nonzero. This means that the quadratic distribution will not accurately represent sharply varying quantities. The quadratic distribution will exhibit a dissipated or viscous distribution and will not vary as rapidly as the physical variation. When the quadratic distribution is used to determine how much of the conserved quantity the fluxed material carries from the donor to the acceptor zone, the computation value will be less than the true value. For the case of material moving diagonally to the zone faces, material will be transported between the original donor zone and the ultimate acceptor zone in two steps in two dimensions and in three steps in three dimensions. Each of these advection steps will contribute its own dissipation. Contrast this diagonal material motion in one part of the mesh with zone-aligned motion in another portion of the mesh. In the grid-aligned flow, the material will move in a single advection step from the donor to the acceptor zone and will thus experience less dissipation.

Van Leer Method

As mentioned above, most Eulerian codes calculate the transported value of the conserved quantities using the van Leer methodology. As a review, in one spatial dimension van Leer approximated a distribution on a uniform grid using a quadratic function. One implementation writes the quadratic function over the interval $\left(x_i, x_{i+1}\right)$, using its centroid $\bar{x}$, as:

$$f(x) = \bar{f} + \overline{\Delta} f\left(\frac{x-\bar{x}}{\Delta x}\right) + \frac{1}{2}\overline{\Delta}^2 f\left[\left(\frac{x-\bar{x}}{\Delta x}\right)^2 - \frac{1}{12}\right], \tag{1}$$

where $\bar{f}$ is the cell mean, $\overline{\Delta} f$ is the limited first spatial difference (Fig. 1), and $\overline{\Delta}^2 f$ is a second difference of the quantity $\bar{f}$. The calculation of the limited first difference involves consideration of three different numerical differences, as illustrated in Fig. 1. All three alternatives are calculated, and the difference with the minimum magnitude is used. To ensure that no new maxima or minima are created, if

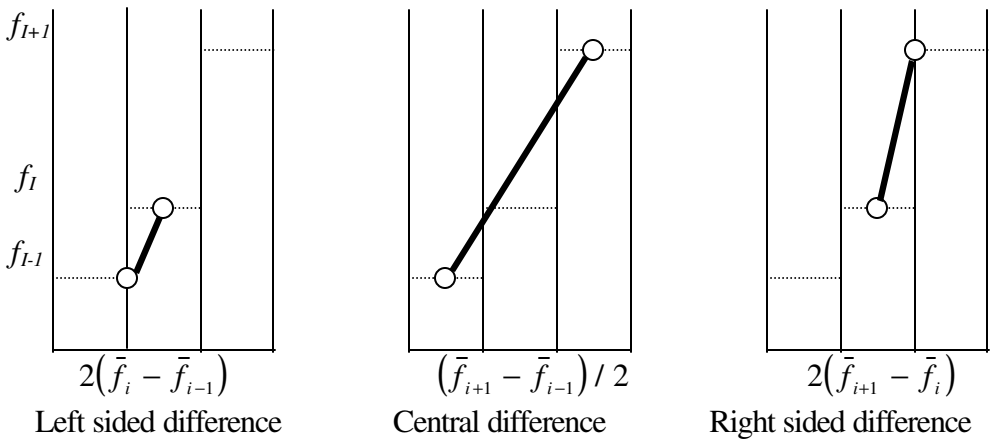

Figure 1. One-dimensional van Leer difference choices for spatial difference of *f*.

the sign of the left and right differences is different, the resulting difference is zeroed. In a similar way, the second difference

$$\overline{\Delta}^2 f = (\overline{\Delta} f_{i+1} - \overline{\Delta} f_{i-1}) \quad (2)$$

was calculated and then adjusted so that the interpolated values at the zone edges do not fall outside the range of values of $\bar{f}$ over the three zones. To perform this limiting, Eq. (1) was used to calculate an interpolated value of f at the zone boundary. If the value of the interpolant fell outside the bounding range of the two $\bar{f}$ s, the value of the second derivative was reduced until the interpolant fell into the prescribed range.

As an important consideration, the representation (1) of the interpolant guarantees that its integral over the zone will equal $\bar{f}$. This will occur independent of the value used for the first or second differences.

Current Method: Vertex Gradients and Zonal Gradients

The current method was developed with the intention of extending the features of the van Leer method to multiple dimensions, and ensuring that the accuracy of the method would be the primary objective. By accuracy, we mean that the method best preserves the features of the problem for translational advection problems. Another way of defining accuracy would be the method that exhibits the least dissipation. The method should be accurate on structured and unstructured, orthogonal and nonorthogonal, and two- and three-dimensional meshes.

A simple, two-dimensional, nonorthogonal, unstructured mesh is illustrated in Fig. 2. The central zone is labeled c. The centroid of each neighboring zone is indicated as an open circle and a sample vertex of zone c is indicated by the shaded circle. The average gradient around the vertex v is calculated by means of a line integral around it using the divergence theorem. This line integral extends along line segments that join the centroids of its neighboring zones. Each zone contributes (via the

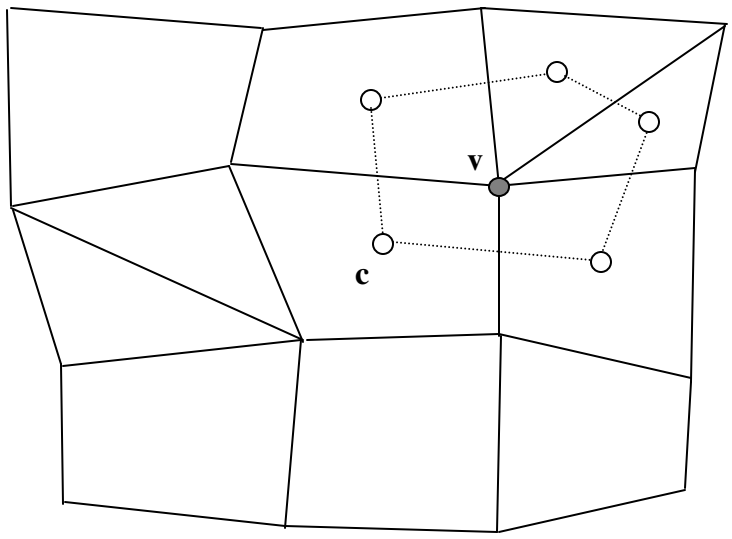

Figure 2. A two-dimensional, nonorthogonal, unstructured mesh.

trapezoidal rule) two terms to the vertex gradient: the zone averages at the segment ends times the segment's exterior normal times the segment length:

$$\nabla f_v = \frac{1}{Vol}\iint \nabla f \; dxdy = \frac{1}{Vol}\oint (f\,\hat{n})dl \cong \frac{1}{Vol_z}\sum_{edges}\left(\frac{\bar{f}_s + \bar{f}_t}{2}\,\hat{n}_e\, l_e\right) \tag{3}$$

John Dukowicz (Dukowicz, 1984) was possibly the first to describe a gradient in this way. Miller and Burton (1990) then implemented Dukowicz's method using a robust and accurate algorithm to compute the gradient. Since we use the trapezoidal rule over a linear segment, if we place a linearly varying quantity over a set of neighboring zones and then calculate the gradient using this method, we reproduce the given gradient to machine roundoff. If we distribute a quadratic function over a mesh, we should do a good job (i.e., convergent) of approximating its average gradient near each vertex. This calculation will be exact for quadratic functions on a tensor product of two uniform one-dimensional meshes and will be convergent for irregular grids.

Recall that van Leer calculated two one-sided differences and a central difference. He examined these to choose the smallest magnitude difference for his limited zonal gradient. In a similar way, we will calculate a gradient at each vertex of the mesh. One extension of van Leer's method to multiple dimensions and convex zones would use the minimum-magnitude vertex gradient for the initially unlimited zonal gradient. Our experience has shown that this choice leads to larger discontinuities in the approximant at the zone edge than occurs with the more flexible limitations we propose below.

In addition to the one-sided gradients, van Leer utilized a central difference. We call our analog of this difference the zonal gradient ∇f_z. To calculate this gradient, first we define a vertex-dual mesh in which segments joining successive neighboring zone's centroids enclose the vertex's dual zone. A vertex's dual zone is the same region that we used for its vertex gradient (Figure 2). Moving around the boundary of an ordinary zone, each vertex zone contributes its vertex gradient and associated vertex volume to the zonal gradient as follows:

$$\nabla f_z = \frac{\sum Vol_v \nabla f_v}{\sum Vol_v}. \tag{4}$$

Due to the cancellation of interior line integrals, this zone-average gradient is the same as the gradient that would be calculated through the line integral formulation (as in Dukowicz and Kodis, 1987) around the cell's surrounding zone centroids. Its magnitude may need to be limited.

In one-dimension van Leer limited the linear approximation to restrict zonal boundary values to lie in the range encompassed by local zones' median values. Dukowicz and Baumgardner (2000) have extended this limiting to multiple dimensions. See also Dukowicz and Kodis (1987) and Swartz (1999) and sections that follow herein.

Hessian Computation

Van Leer approximated the curvature of the interpolation by differencing the two one-sided gradients. In a similar way, we will estimate a zone-centered second derivative by spatially differencing (using the divergence theorem) the vertex gradients around the perimeter of the polygonal zone:

$$\frac{\partial^2 f}{\partial x^2} = \nabla\left(\frac{\partial f}{\partial x}\right)\bullet\hat{i} \cong \frac{1}{Vol_z}\sum_e \bar{f}_x\left(n_x l\right)_e \cong \frac{1}{2Vol_z}\sum_e (fx_s + fx_t)(y_t - y_s)$$

$$\frac{\partial^2 f}{\partial x \partial y} = \frac{1}{2}\left(\nabla\left(\frac{\partial f}{\partial y}\right)\bullet\hat{i} + \nabla\left(\frac{\partial f}{\partial x}\right)\bullet\hat{j}\right) \cong \frac{1}{2Vol_z}\sum_e\left[\bar{f}_y\left(n_x l\right)_e + \bar{f}_x\left(n_y l\right)_e\right] \tag{5}$$

$$\cong \frac{1}{4Vol_z}\sum_e\left[\left(fy_s + fy_t\right)(y_t - y_s) + \left(fx_s + fx_t\right)(x_s - x_t)\right]$$

$$\frac{\partial^2 f}{\partial y^2} = \nabla\left(\frac{\partial f}{\partial y}\right)\bullet\hat{j} \cong \frac{1}{Vol_z}\sum_e \bar{f}_y\left(n_y l\right)_e \cong \frac{1}{2Vol_z}\sum_e (fy_s + fy_t)(x_s - x_t)$$

Here $\bar{f}_x$ and $\bar{f}_y$ are the mean values over the segment of the components of ∇f , and fx and fy are the values of the components of ∇f_v (3) at its endpoints. The subscripts s and t refer to the starting and terminating vertices of the edge. There are two methods for computing the cross-derivative term, both of which produce almost the same result. Our method (5) averages the two alternatives to produce the cross derivative.

This approach provides exact estimates of second derivatives for multivariate quadratic functions on uniform grids. On more irregular grids, however, convergence or even boundedness of the estimates is not to be expected. This is in spite of the fact that the resulting difference formulae yield convergent and second-order-accurate approximations to solutions of ordinary differential equations on irregular grids as the mesh size gets small. For proof of this see Manteuffel and White [1986, esp. Section 5].

The following analysis demonstrates these problems in one space dimension. Let four mesh vertices bound three adjacent mesh cells that have centroids $\bar{x}_1, \bar{x}_2, \bar{x}_3$ and mesh widths h_1, h_2, h_3 respectively. Apply our approach to the three successive cell means $\bar{f}_1, \bar{f}_2, \bar{f}_3$. Our estimates for the two successive vertex-centered gradients are $\left(\bar{f}_{i+1} - \bar{f}_i\right) / \bar{h}_{i+1/2}$ where $\bar{h}_{i+1/2} = \left(h_i + h_{i+1}\right)/2$. Integrating Taylor expansions about the $\bar{x}_i$ shows these numbers are within $O(h^2)$ of $f'\left(\bar{x}_{i+1/2}\right)$, where $\bar{x}_{i+1/2} = \left(\bar{x}_{i+1} + \bar{x}_i\right)/2$. Thus, they are convergent but not second-order accurate approximations of the value of the first derivative f' at other locations (in particular, at the cell vertices $x_{i+1/2}$). Turning to f'', the distance between the two middle vertices being h_2, our proposed estimate of the second derivative is the number

$$\left[\left(\bar{f}_3 - \bar{f}_2\right) / \bar{h}_{5/2} - \left(\bar{f}_2 - \bar{f}_1\right) / \bar{h}_{3/2}\right] / h_2 .$$

But: h_2 can be quite different from $\bar{x}_{5/2} - \bar{x}_{3/2}$ and, since the use of the latter would be convergent, the use of the wrong value, h_2, can yield a nonconvergent estimate, even an unbounded one if adjacent mesh sizes vary wildly (e.g., take $h_1 = h_3 = h, h_2 = h^2$).

Limiting the Zonal Gradient

The quadratic distribution should not produce new internal maxima or minima so that instabilities or noise in the zonal median values are not amplified. Van Leer set the gradient to zero if the signs of the one-sided differences were different, and we employ a similar check. We computed a gradient at each mesh vertex. For each zone we compute the dot product of each vertex's gradient with all of the zone's

other vertex gradients. If any of the products is negative, the gradient around the zone's perimeter would have components in opposite directions. In this instance we set the zone's gradient to zero.

Quadratic Expression

The quadratic expression we use to describe the distribution over a zone is

$$f(x,y) = \bar{f} + f_x(x-\bar{x}) + f_y(y-\bar{y}) + \tfrac{1}{2} f_{xx}\left[(x-\bar{x})^2 - Avg[(x-\bar{x})^2]\right] + f_{xy}(x-\bar{x})(y-\bar{y}) + \tfrac{1}{2} f_{yy}\left[(y-\bar{y})^2 - Avg[(y-\bar{y})^2]\right]. \quad (6)$$

Here $\{\bar{x},\bar{y}\}$ is the zone's centroid and $Avg\left[g(\,)\right]$ is the mean value of the function $g(\,)$ over the zone. These terms guarantee that when this expression is integrated over a polyhedral cell, its value will be $\bar{f}$, the mean zone value, times the volume of the polyhedron. This makes the distribution conservative; i.e., $\bar{f}_z V_z$ is $\int f\, dV$ for each zone *z*.

Gradient and Hessian Limiting

Van Leer employed his one-dimensional, quadratic function to limit the interpolated value of the function at the two zone boundaries. In a similar way, we limit the value of the interpolant on the line between the home zone's centroid and each neighboring zone's centroid. For each neighbor we will require the associated boundary value of the interpolant to lie between the mean value $\bar{f}$ for the home zone and $\bar{f}$ for the neighboring zone.

Let the zone's centroid *C* be at $\{\bar{x},\bar{y}\} = \{C_x, C_y\}$. The five nonconstant functions

$$x - Cx, \quad y - Cy, \quad \frac{1}{2}\left\{(x-Cx)^2 - Avg\left[(x-Cx)^2\right]\right\}, \quad (x-Cx)(y-Cy), \quad \frac{1}{2}\left\{(y-Cy)^2 - Avg\left[(y-Cy)^2\right]\right\} \quad (7)$$

in (6) may be viewed as the basis for a five-dimensional vector space V_5. All members of V_5 have mean value zero over the zone. Given a number $\bar{f}$, the set of functions in V_5 that all have the value $2-\bar{f}$ at a given fixed point $x=a$ and $y=b$ constitute a four-dimensional hyperplane $P(a,b,2-\bar{f})$ in V_5. So given also the constant function 1 the functions of the form (6) that have mean value $\bar{f}$ and also have value 2 at {*a,b*} are exactly the functions in $\bar{f}\times 1 + P(a,b,2-\bar{f})$. $P(a,b,c)$ divides V_5 into two five-dimensional half-spaces: namely, the functions that exceed *c* at the point{*a,b*} and the functions that are less than c at {*a,b*}. Such linear inequality constraints on elements in V_5 correspond to five-dimensional half-spaces of V_5, and the functions that satisfy a number of such constraints consist exactly of the functions in the intersection of the corresponding half-spaces. Intersections of half-spaces constitute convex polyhedra in V_5.

Having suitably normalized each element in the above basis for V_5, we may take as coordinates for V_5 the five derivative values $f_x(C), f_y(C), f_{xx}(C), f_{xy}(C), f_{yy}(C)$. Having defined some coordinates, we can minimize the distance (as measured by summed squared coordinate differences) that we are from a given point of V_5 and still lie in a given polyhedron. This is the essence of what we propose to do – and what O'Rourke and Sahota (1998) did for vertex values of gradients.

Constraint Enclosure Construction

For each zone, we wish to construct a monotonic interpolant of a zone's mean value *fh*. To do so we restrict variation towards each neighboring zone's centroid using that neighboring zone's mean value *fn* as follows. Let the point *Pn* lie at the intersection of the home cell's boundary with the line segment that joins the home cell's centroid *Ch* to a given neighboring zone's centroid *Cn*. With each function *g* in V_5 is an associated value *g(Pn)*, and the function *fh+g* has value *fh+g(Pn)* there. We want to restrict ourselves to those quadratics whose values at *Pn* lie between the numbers *fh* and *fn*. Thus, we want to restrict ourselves to those elements of V_5 whose values at *Pn* lie between zero and *fn-fh* (this is related to the so-called "MUSCL" constraint.) Towards this end, let *N* be the five-vector of values at *Pn* of the five basis vectors (7). That is to say, if

$$Bn = Pn - Cn$$

$$N = \left\{ Bnx,\ Bny,\ \frac{1}{2}\left[Bnx^2 - Avg\left((x - Chx)^2 \right) \right],\ Bnx\ Bny,\ \frac{1}{2}\left[Bny^2 - Avg\left(\left(y - Chy \right)^2 \right) \right] \right\}$$

Then the hyperplane of vectors *D* in V_5 satisfying the equality constraint

$$N \bullet D = 0$$

are those five-vectors of derivatives at *Ch* of the functions of the form (6) that have value *fh* at the boundary point *Pn* between the two centroids. Likewise, the vectors *D* satisfying the constraint

$$N \bullet D = fn - fh$$

are the derivatives of the functions (6) having the value *fn* at *Pn*. Each vector in the slab *Sn* lying between these two parallel hyperplanes in V_5 corresponds to a function of the form (6) having a value at *Pn* lying between *fh* and *fn*.

Each neighboring zone of the given home zone has its own zone mean, its own intermediate point *Pn*, and its own associated slab *Sn* that constrains potential vectors *D* of allowable derivative values at the home zone's centroid. We ask that the constraints for all neighbors take effect simultaneously (this amounts to a directional weakening of the "MUSCL" constraint used by Dukowicz and Kodis and is an analog of O'Rourke and Sahota in our more general context). Geometrically this intersection of the slabs *Sn* corresponding to all the neighboring zones yields our polyhedral constraint enclosure *E*. Since the slabs are convex sets, *E* is a closed convex subset of V_5.

We shall use *E* to limit some given estimate

$$F = \{ f_x, f_y, f_{xx}, f_{xy}, f_{yy} \}$$

of numbers for the derivatives at the home zone's centroid as follows: if *F* does not lie in the constraint enclosure *E*, we use the nearest vector in *E* instead. For 'nearest' here, we follow O'Rourke and Sahota and use the Euclidean distance between the coordinates.

An Example Constraining Linear Functions

Dukowicz and Baumgardner (2000) presented an interesting problem: a circular distribution of height 1 is imposed upon a background of 0.1, and this distribution is then transported around the mesh's center point. This problem is a challenge because of the discontinuity in the distribution as well as the spatial curvature of the step. This problem was used extensively in the development of the current work. To illustrate this method, let us look at a portion of the mesh near the discontinuity in Fig. (3) and consider limiting a linear (not quadratic) function *f*. The space of derivative values is now two-dimensional.

The central zone *h* is shown with its eight neighbors *n1* through *n8*. The average zone value is indicated next to its letter identifier. The constraints associated with neighbor *n1* are shown in Fig. (4) and neighbor *n3* in Fig. (5). In Fig. (6), the constraints are collected into one plot. The monotonicity constraint slabs that the neighboring zones impose are bounded by heavy lines. The average, unlimited zonal gradient for the home zone is indicated as the red-filled circle (near 'n1'). The limited gradient (the blue-filled circle near the origin) is 'interior' to the constraint enclosure.

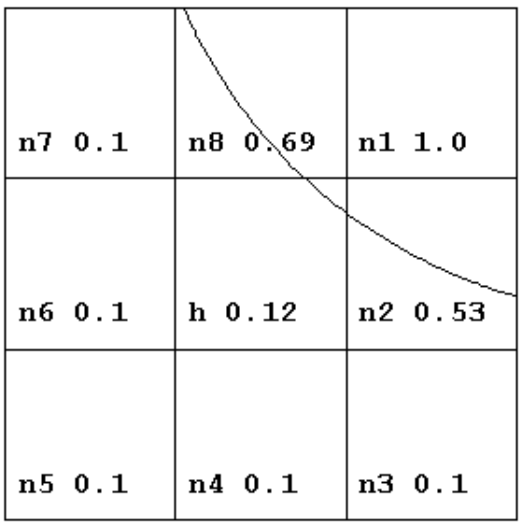

Figure 3. Portion of mesh from Dukowicz and Baumgardner's circular step problem.

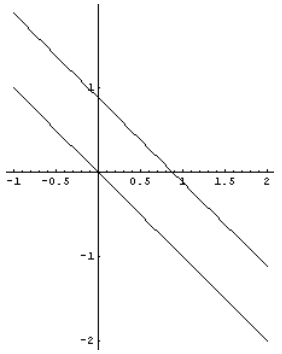

Figure 4. *n1* constraints

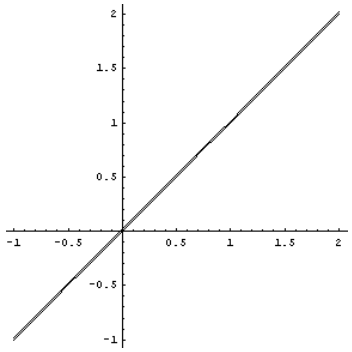

Figure 5. *n3* constraints

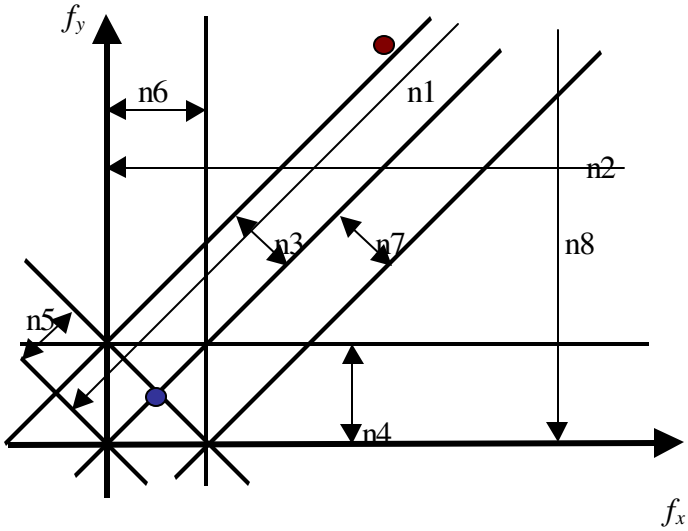

Figure 6. Limits on gradient of linear functions.

In this example, the constraint enclosure E is unusual in that it has zero area because of the *n3* and *n7* constraints. In other problems, where the area in the constraint enclosure is more extensive, the question of how to determine the limited values of the gradient and Hessian at the centroid is less straightforward. To summarize, the criteria that this work uses to determine the limited quadratic are that:

- the derivatives (coordinates) must be interior to all constraints,
- the Euclidean distance of the coordinates from those of the original input derivative estimates is to be a minimum.

There are a number of other objective functions that could be used to select among the constrained quadratic functions.

Limiting Procedure

We seek the unique vector L that is closest to F (in the Euclidean distance) while still satisfying all the inequality constraints; i.e., the vector L lies in the convex constraint polyhedron E. The process of limiting the gradient and Hessian values could be broken into two successive steps. We might first limit the gradient and then, using these values for the gradient, limit the Hessian. It was found that breaking the monotonicity limiting into two successive steps resulted in a less dynamic representation (the components of the Hessian were reduced or eliminated). The gradient limiting "used up" the range of values allowed by the monotonicity. When the gradient and Hessian were limited simultaneously, the components of the Hessian that resulted produced a more curved interpolant.

This is a minimization problem involving a quadratic objective function subject to linear constraints. We solve it following the "Gradient Projection Method" in Fox (1973) that produces a finite sequence of points $Li,\ i=1,2,\ldots$ that lie in E, with each element closer to F than the last. The sequence terminates at L. First, if F itself violates no constraints, then $L=F$. Otherwise, we begin with $L_1 = 0$ since it lies in E. Then L_2 is taken to be that point on the part of the line $L_1 + s(F-L_1)$ lying in E that is closest to F. Since E is convex, L_2, and its successors in the sequence, lies in E's boundary, B. At L_2 we select the j_2 constraint(s) that is (are) exactly satisfied (equality, not inequality)—i.e., that are active at L_2. Our next motion will take place along a line segment lying in some of the associated hyperplanes $H_{2,j},\ j=1,..,j_2$. Roughly speaking, we want to move from L_2 in the descent direction L_2-F (i.e., opposite to the direction of the local value of the objective function's gradient) as best we can but still remain in the boundary B. We should be able to do this by removing from L_2-F its component in the span of the hyperplanes' j_2 normal vectors. It is a tricky business as not all the constraints active at L_2 may be usable in the desired direction from L_2. We are not allowed to exit the constraint enclosure, so the active constraints with a positive inner product between its normal and the descent direction are collected. There may be several active constraints that are restricting motion. To determine a descent direction along B, we carefully use the projection matrix that Fox described. This projection step is complex and requires careful attention; it either produces a direction that remains interior to the enclosure or produces a vector with zero length. The zero-length vector indicates that no further interior motion is possible; the optimum value for L has been reached and it minimizes the objective function. If the projected direction is non-zero, motion interior to the enclosure is possible; however, the distance to the nearest inactive constraint will limit the step length. The distance to all nonactive constraints along the projected direction is calculated. We place the next point L_3 in the sequence at the minimum of these distances, except that—as the segment we're moving on lies in the boundary of the polyhedron E—the even more

desirable point minimizing the distance from F to the segment may be reached first. The process is then repeated to yield points $L_4, L_5, \ldots$ until no motion in E that has any component in F's direction is possible.

A Smooth Limiting Example

To illustrate the accuracy of the results, a smooth, high-order function is imposed on a uniform, orthogonal grid. This test function is a cosine wave radially propagating from the origin with a circular distribution:

$$f(x, y) = \cos\left(\frac{x^2 + y^2}{6}\right). \tag{8}$$

The resulting, limited piecewise quadratic distribution is illustrated in Fig. (7), in which each of the 25 zones is 1 by 1. The lower left corner of the graphic starts at the coordinate {-4,-4} and the upper right corner is at {1,1}. To illustrate the distribution's curvature, each zone has a 4 by 4 mesh imposed upon it. The first circle upon which the input function takes its minimum value passes near {-3,-3}. This

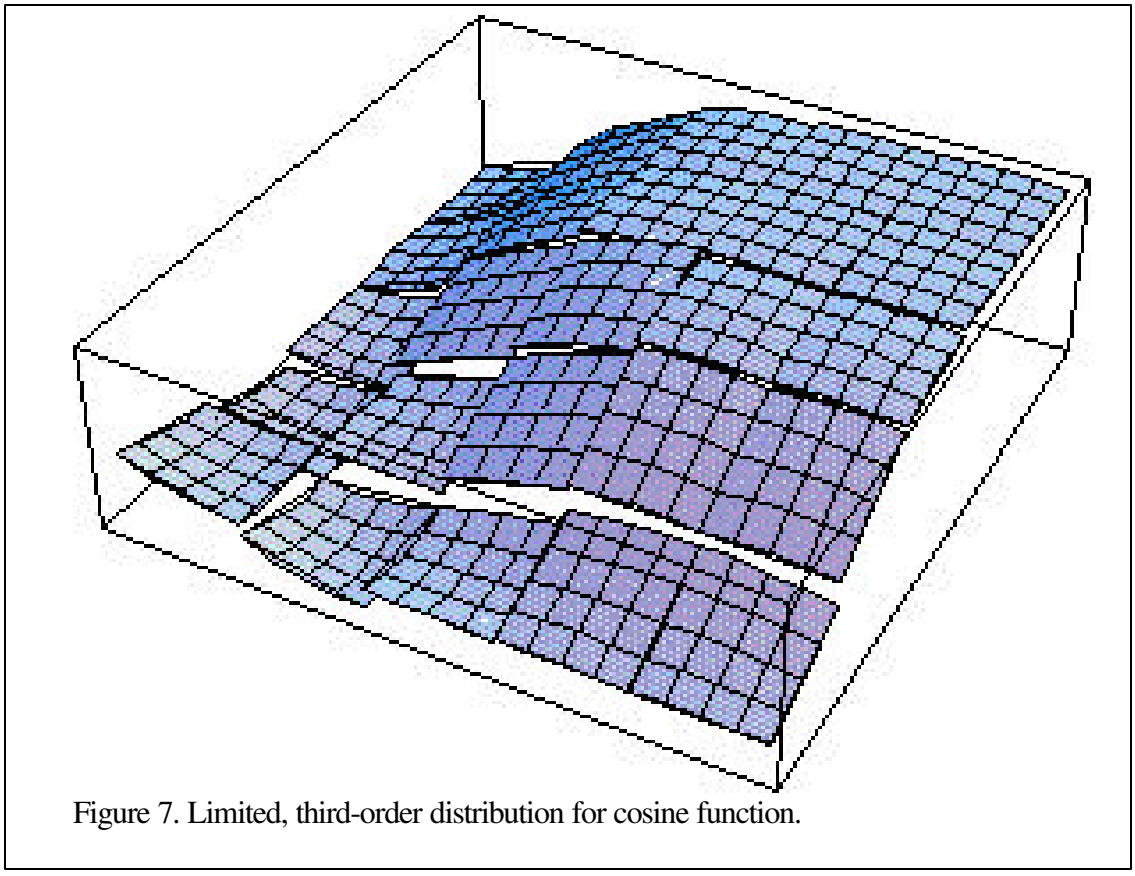

Figure 7. Limited, third-order distribution for cosine function.

behaviour also occurs in the interpolant.

The interpolant follows the input function very accurately. Fig. (8) is a plot of the same function locally approximated by similarly limited linear functions. The limiting process used to compute the interpolants in Fig. (8) included only the constant and linear terms as in O'Rourke and Sahota. The continuity of the interpolant between neighboring zones is significantly decreased.

A useful error measure is the absolute value of the difference between the analytic cosine function (8) and the interpolant. The analytic expression for the mean absolute error over a zone is not available.

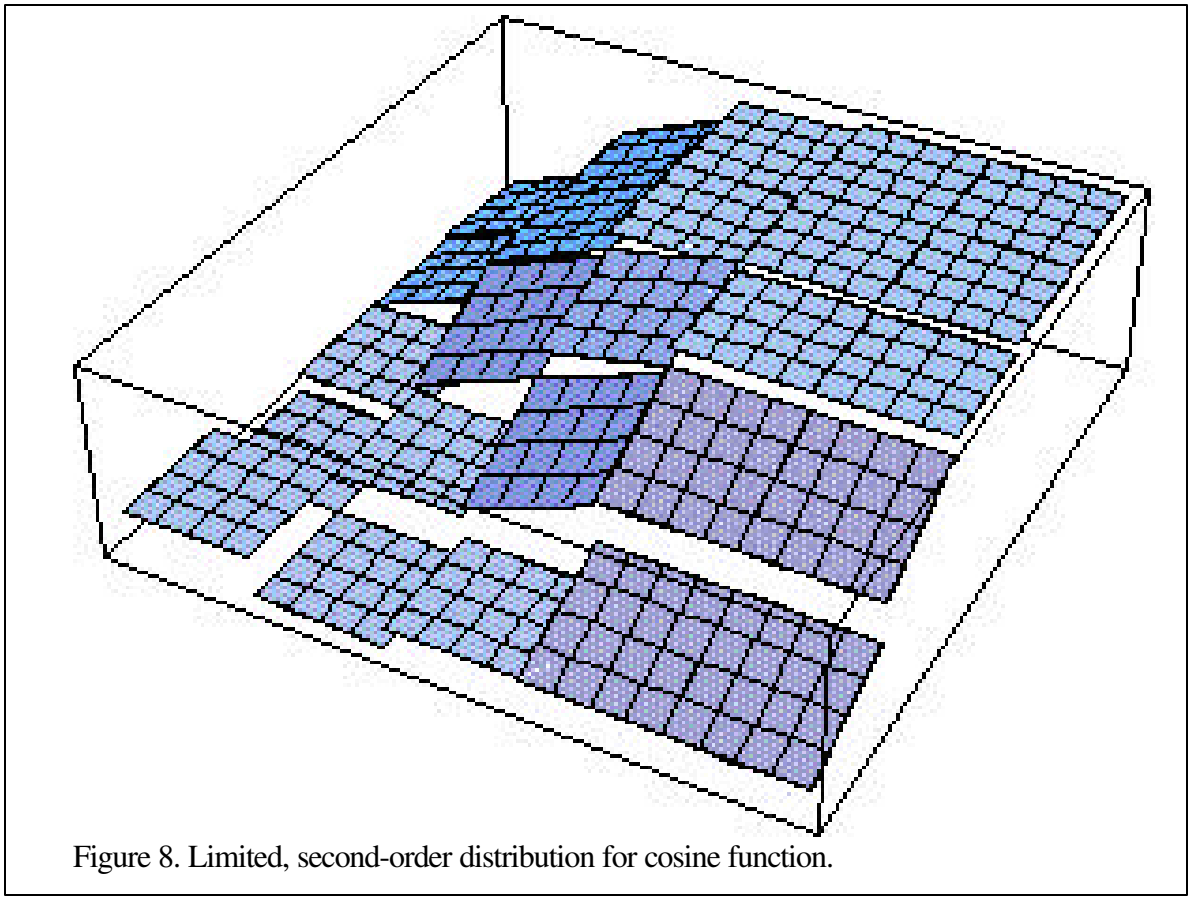

Figure 8. Limited, second-order distribution for cosine function.

An approximation is computed by sampling the error at a number of locations in each zone and averaging the sum. Twenty-five, evenly spaced locations were chosen in each zone and the mean absolute error was computed for the second-order and the third-order interpolant. Fig. (9) is a histogram comparing these two errors. The red bars are the second-order interpolant mean absolute error and the blue bar is the mean absolute error for the third-order interpolant. The range of errors in Fig. (9) is 0.064 in the lower left corner to 0.003 in the upper right corner. In areas of the problem where the cosine function has small changes between neighboring zones, both second- and third-order interpolants do a good job of representing the function. In regions of significant curvature, the third-order interpolant produces a more continuous representation of the function between adjoining zones as well as a lower error. Since advection transports material from the edge of one zone to another, the more continuous representation by the third-order interpolant will produce a less diffusive advection step that may better preserve features of the problem.

Conclusions

A piecewise quadratic method of representing the distribution of a conserved quantity has been developed. The method more accurately represents the spatial distribution of these quantities and should enable an unsplit advection algorithm to more accurately transport material. The interpolant is monotonic with respect to its immediate neighboring zones in a MUSCL sense. A more extensive examination of

the relationship between extrema of the approximant and monotonicity needs to be considered in the future.

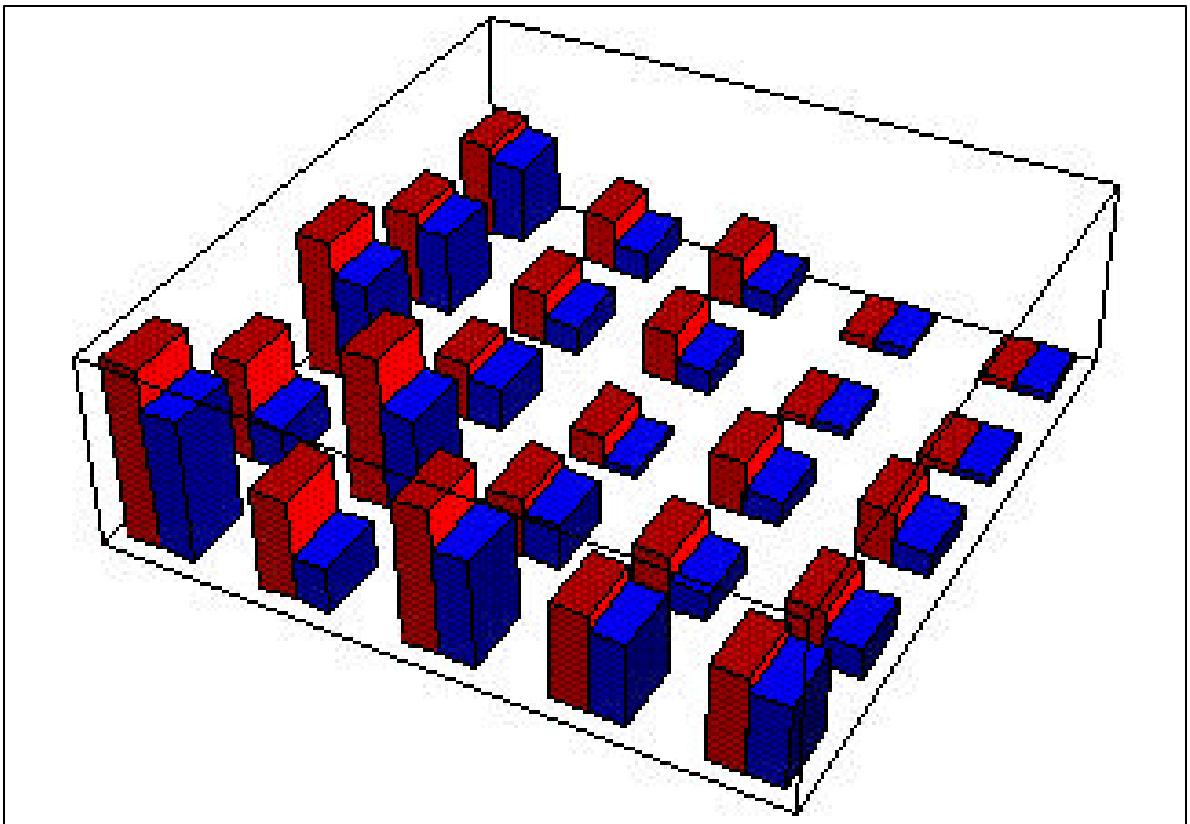

Figure 9. Histogram of average second- and third-order errors.

References

Boris, J.P. and Book, D.L., JCP, **11**, 38- (1973).

Dukowicz, J.K., "Conservative Rezoning (Remapping) for General Quadrilateral Meshes," JCP, **54**, 411-424 (1984).

Dukowicz, J.K. and Baumgardner, J.R., "Incremental Remapping as a Transport/Advection Algorithm," JCP, **160**, 318-335 (2000).

Dukowicz, J.K. and Kodis, J.W., "Accurate Conservative Remapping (Rezoning) for Arbitrary Lagrange-Eulerian Computations," SIAM J. Sci. Stat. Comput., **8**, 305-321 (1987).

Fox, R.L., *Optimization Methods for Engineering Design* (Addison-Wesley, 1973).

Manteuffel, T. A. and White, A. B., "The Numerical Solution of Second-Order Boundary Value Problems on Nonuniform Meshes," Math. Comp., **47**, 511-535 (1986).

Miller, D. S., Burton, D.E., Oliviera, J. S., "Efficient Second Order Remapping on Arbitrary Two Dimensional Meshes," UCRL-ID-123530.

O'Rourke, P.J. and Sahota, M.S., "A Variable Explicit/Implicit Numerical Method for Calculating Advection on Unstructured Meshes," JCP, **143**, 312-345 (1998).

Rider,W.J. and Kothe, D.B., "Reconstructing Volume Tracking," JCP, **141,** 112-152 (1998)

Swartz, B.K., "Good Neighborhoods for Multidimensional Van Leer Limiting," JCP, **154**, 237-241 (1999).

Van Leer, B., "Towards the Ultimate Conservative Difference Scheme. IV. A New Approach to Numerical Convection," JCP, **23**, 276-299 (1977).

Acknowledgements

This work was performed under the auspices of the U.S. Department of Energy by the University of California Los Alamos National Laboratory under contract No. W-7405-Eng-36.